Collisional Quenching of Hg_2 (AO_g^+)

Z. G. Figen, H. C. Tran,† and J. G. Eden*

Everitt Laboratory, Department of Electrical and Computer Engineering, University of Illinois, Urbana, Illinois 61801

Received: January 23, 1998; In Final Form: March 25, 1998

The rate constants for quenching of the metastable AO_g^+ state of Hg_2 in two and three body collisions with background Hg atoms have been measured by a pump−probe, laser-induced fluorescence technique. The Hg_2 (AO_g^+) species was produced by photoassociating thermal Hg−Hg pairs at 266 nm which populates the $D1_u$ level of Hg_2. Subsequent collisions relax the dimer into the AO_g^+ state. The temporal history of the A state number density was monitored by driving the $GO_u^+ \leftarrow AO_g^+$ transition in the yellow ($\lambda \sim 564$ nm) and observing $GO_u^+ \rightarrow XO_g^+$ emission in the ultraviolet ($\lambda \sim 210-240$ nm). The two and three body rate constants for quenching of Hg_2 (AO_g^+) by Hg were measured to be $(4.5 \pm 3.0) \times 10^{-15}$ cm^3·s^{-1} and $(1.8 \pm 0.4) \times 10^{-33}$ cm^6·s^{-1}, respectively.

A. Introduction

The lowest-lying electronic excited states of the mercury dimer, denoted in Hund's case (c) coupling notation as $O_g^\pm$, are metastable with respect to the O_g^+ ground state and, as noted by Mies et al.,[1] "...function only as reservoir states..." It is not surprising, then, that several attempts have been made to extract energy stored in the $O_g^\pm$ or nearby 1_u states. Efforts in the 1970s to obtain lasing on the $1_u \rightarrow O_g^+$ transition of Hg_2, which gives rise to the well-known continuum peaking at ~335 nm, were unsuccessful, presumably because of excited state absorption. Mosburg and Wilke[2] and Ehrlich and Osgood[3] subsequently reported experiments in which the extraction of energy from Hg_2 ($O_g^\pm$) by pumping 1_u, $O_u^\pm \leftarrow O_g^\pm$ transitions with an infrared chemical laser was investigated and, recently, Figen et al.[4] attempted to obtain stimulated electronic Raman scattering in Hg_2 by an anti-Stokes process in which the AO_g^+ and GO_u^+ states serve as the initial (energy storage) and intermediate states, respectively.

An obstacle to utilizing the AO_g^+ state was that, until the mid 1980s, "...the existence of the gerade metastable levels [of Hg_2 had] not been established spectroscopically".[1] In a series of laser-induced fluorescence experiments, Krause and coworkers[5−9] identified the G, H, I ← A transitions of Hg_2, determined vibrational constants for each of the electronic states involved in these transitions, and subsequently resolved rotational structure in the G ← A band.[10]

In this paper, the measurement of the rate constants for quenching of Hg_2 (AO_g^+) in two and three body collisions with background Hg atoms by a laser pump−probe technique is described. Dimers in the A state are produced by the photoassociation of Hg−Hg pairs to initially populate the Hg_2 ($D1_u$) level which subsequently is deactivated by collisions with background Hg ($6\ ^1S_0$) atoms. The temporal history of the relative Hg_2 (A) number density is monitored by photoexciting the (v', v'') = (9, 0) band of the Hg_2 (G ← A) transition and monitoring the ensuing emission on the G → X transition of the dimer.

B. Experiments

A partial energy level diagram of Hg_2 illustrating the electronic states of interest is given in Figure 1. In these experiments, photoassociating pairs of thermalized Hg($6s\ ^1S_0$) atoms[11,12] at 266 nm produces the Hg_2 $D1_u$ excited species,[13,14] and subsequent collisions with ground-state Hg atoms populate the AO_g^+ state. As will be discussed later, relying on formation of the A state by collisions inherently limits the range in Hg number densities over which useful measurements can be made. Exciting the $GO_u^+ \leftarrow AO_g^+$ transition of the dimer with a time-delayed optical pulse results in $GO_u^+ \rightarrow XO_g^+$ emission in the ultraviolet ($210 \lesssim \lambda \lesssim 240$ nm) which provides a convenient measure of the relative AO_g^+ number density. By varying the time delay between the pump (266 nm) and probe ($\lambda \sim 564$ nm) pulses, the temporal decay of the AO_g^+ population can be recorded. Note that, because of parity considerations, only the AO_g^+ population is sampled in these experiments. However, the adjacent O_g^- level undoubtedly acts as a reservoir that is closely coupled to O_g^+ by collisions.

A schematic diagram of the experimental arrangement is shown in Figure 2. Ground-state Hg−Hg pairs are photoexcited by optical pulses (~5 ns full width at half-maximum (fwhm), 5 mJ, 10 Hz) from a frequency-quadrupled Nd:YAG laser. The 266 nm beam is overlapped inside a quartz cell, (2.5 cm diameter (o.d.), 10 cm in length) with radiation from an Nd:YAG-pumped dye laser. Tunable over the 556−580 nm region, the dye laser (probe) pulses have temporal and spectral widths of ~10 ns and ~0.2 cm^{-1}, respectively, and have energies of nominally 10 mJ. The time delay (Δt) between the pump (266 nm) and probe pulses can be adjusted continuously by a time delay generator. As has been noted by Drullinger et al.,[13] quenching of electronically-excited Hg_2 by oxygen and other gases is efficient, so care must be taken in preparing the optical cells. After evacuating the optical cell and outgassing at a base pressure of 10^{-7} Torr, Hg was admitted to the cell which was then sealed off under vacuum. The cell was heated in an oven and its temperature maintained to within ±1 °C. The G → X fluorescence in the ultraviolet (UV) was monitored at a right angle to the optical axis (defined by the pump and probe beams)

† Present address: Northrop-Grumman, 600 Hicks Rd, Rolling Meadows, IL 60008.

S1089-5639(98)00873-1 CCC: $15.00
Published on Web 06/05/1998

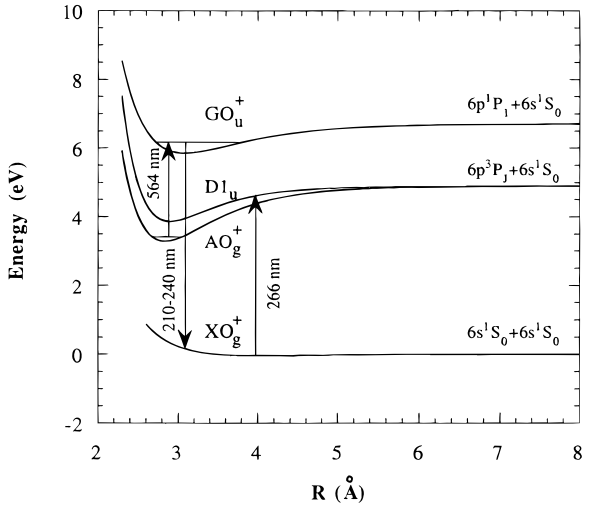

Figure 1. Partial energy level diagram for Hg_2 illustrating qualitatively the electronic states and processes of primary interest to these experiments. Spectroscopic constants for the AO_g^+ and GO_u^+ states of the dimer can be found in ref 10. A review of theoretical and experimental studies of the ground (XO_g^+) state is given in ref 15.

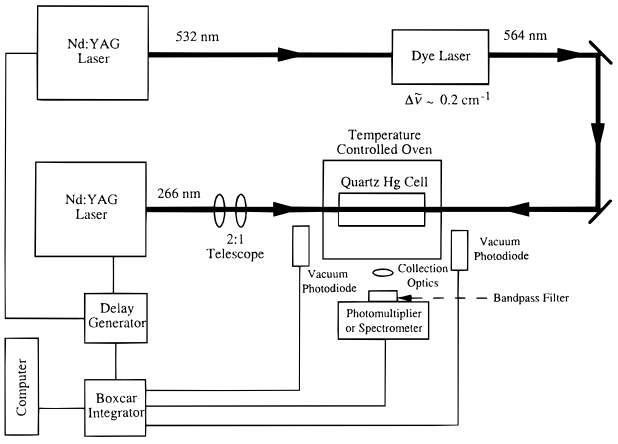

Figure 2. Schematic diagram of the experimental arrangement.

by a photomultiplier and either a bandpass filter (214 ± 6 nm) or a 0.25 m monochromator operated in first order. The fluorescence signals were sampled by a boxcar integrator with a 20 ns gate, and fiducial markers were provided by detecting scatter from both the probe and pump pulses with vacuum photodiodes. The entire experiment was under the control of a computer which recorded the relative intensity of the spectrally-integrated G → X emission as Δt was scanned (which required moving both the probe pulse and boxcar integrator gate synchronously with respect to the pump pulse).

C. Results and Discussion

Condon internal diffraction spectra of the G → X transition of Hg_2 are readily produced by exciting specific rovibrational transitions of the $GO_u^+(v') \leftarrow AO_g^+(v''=0)$ bands with the probe radiation. As an example, Figure 3 shows the bound → free emission observed when the $(v', v'') = (9, 0)$ transition of the G ← A band is driven at 564 nm. Similar spectra have been observed previously for Hg_2[5−7] and are representative of those reported for the other group IIB metal dimers (Zn_2 and Cd_2).[12]

Figure 4 presents data representative of those obtained at 20 values of Hg number density (i.e., cell temperature). These results reflect the temporal decay of the Hg_2 (A) state population and, as expected, the decline of the A state number density

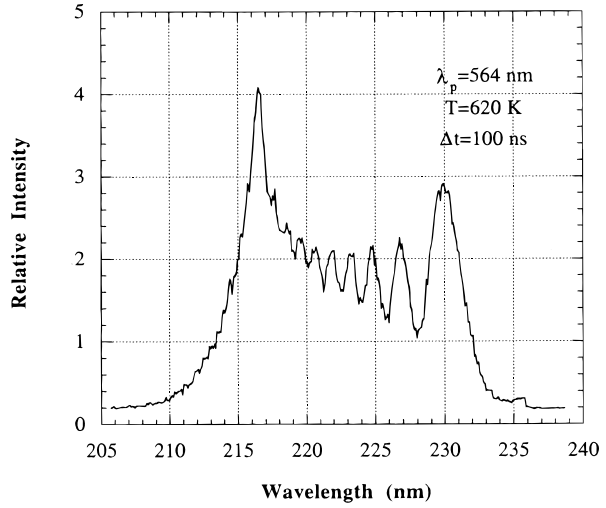

Figure 3. Hg_2 (G → X) bound → free emission spectrum observed when the $AO_g^+ \rightarrow GO_u^+$ transition is pumped at 564 nm which corresponds to excitation of the $(v', v'') = (9, 0)$ band. The time delay between the 266 nm (pump) and probe laser pulses is 100 ns.

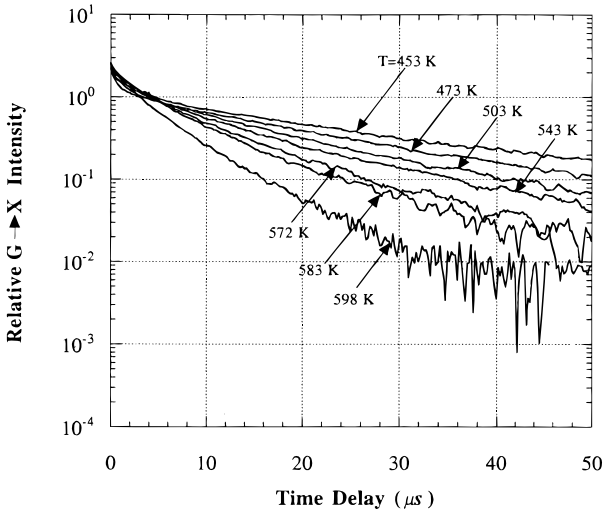

Figure 4. Representative data illustrating the decay of the relative AO_g^+ population following the pump pulse. For clarity, only the results obtained at seven temperatures are shown.

accelerates as the background Hg concentration is increased. A simple rate equation description of the Hg_2 (A) population in the aftermath of the photoassociation pulse reproduces well the experimental results. The temporal history of the A state number density following the 266 nm pulse can be expressed as

$$\frac{d}{dt}[Hg_2(A)] = k_1[Hg][Hg_2(D)] - \{\tau_{sp}^{-1} + k_2[Hg] + k_3[Hg]^2\}[Hg_2(A)] \quad (1)$$

where square brackets denote number densities, τ_{sp} is the spontaneous emission lifetime for the A state, and k_2 and k_3 are the rate constants for quenching of Hg_2 (AO_g^+) in two and three body collisions, respectively, with background Hg ($6\,^1S_0$) atoms. Note that eq 1 assumes that the AO_g^+ state is formed directly from $D1_u$ by two body collisions. Furthermore, collisions between excited species (Hg_2 (A) − Hg_2 (A)) have been ignored. This process introduces a term into eq 1 that is quadratic in the Hg_2 (AO_g^+) number density. Recalling that the Hg−Hg pair photoassociation rate varies as the square of [Hg] and that the absorption coefficient at 266 nm is small (~10^{-39}

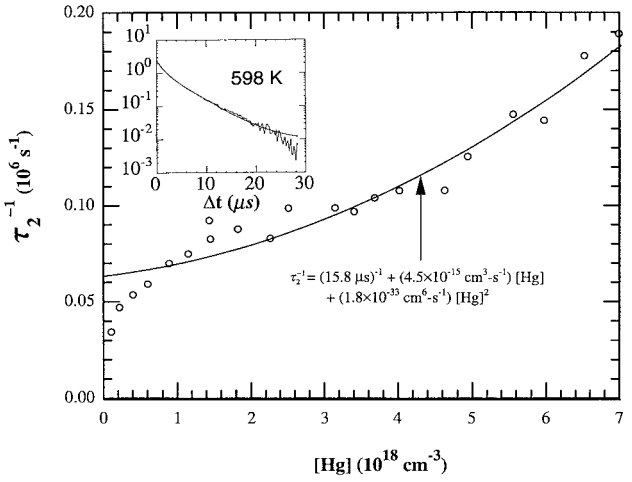

Figure 5. Dependence of the exponential decay rate, τ_2^{-1}, on the Hg number density. The solid curve is the least-squares fit of the second-order polynomial, $\tau_2^{-1} = \tau_{sp}^{-1} + k_2[\mathrm{Hg}] + k_3[\mathrm{Hg}]^2$ (eq 3) to the [Hg] $> 5 \times 10^{17}$ cm^{-3} data. The inset shows a comparison of the experimental trace for $T = 598$ K with the best fit of eq 2 to the data.

cm^5),[13] then the fractional excitation of Hg atoms is negligible ($<10^{-3}$), even for the highest Hg number densities studied in these experiments. Consequently, the impact of Hg_2 (A)−Hg_2 (A) collisions on eq 1 may be neglected for the experimental conditions of interest.

If the Hg number density, [Hg], is sufficiently large that the AO_g^+ formation time is small relative to the inverse of the collisional loss rate, then the source term in eq 1 can be neglected for the moment and the decline of the Hg_2 (A) population is given by

$$[\mathrm{Hg_2\,(A)}] = Ae^{-t/\tau_1} + Be^{-t/\tau_2} \qquad (2)$$

where A and B are constants,

$$\tau_2^{-1} = \tau_{sp}^{-1} + k_2[\mathrm{Hg}] + k_3[\mathrm{Hg}]^2 \qquad (3)$$

and k_2 and k_3 are expressed in units of cm^3•s^{-1} and cm^6•s^{-1}, respectively. All of the Δt scans (similar to those of Figure 4) were fit to eq 2 by computer, and τ_2 was determined. The results are summarized in Figure 5 in which τ_2^{-1} is shown as a function of [Hg] for mercury number densities $\leq 7 \times 10^{18}$ cm^{-3}. The inset compares the experimental Δt data for $T = 598$ K with the least squares fit of eq 2.

Interpretation of the data of Figure 5 requires that we first consider the behavior of the system at low Hg number densities. It is apparent that, for [Hg] $\lesssim 5 \times 10^{17}$ cm^{-3}, the formation of Hg_2 (A) is the limiting process and the data are consistent with a two body $1_u \rightarrow O_g^+$ formation rate constant of 3×10^{-14} cm^3•s^{-1}. Said another way, collisional mixing between the AO_g^+ and $D1_u$ states dictates the temporal history of the A state population in this low Hg density region. Consequently, only those data obtained for [Hg] $> 5 \times 10^{17}$ cm^{-3} were analyzed to determine the AO_g^+ quenching rate constants. It is interesting to note that the two body rate constant mentioned above is smaller than, but comparable to, the rate constants for collisional relaxation of Hg ($6\ ^3P_1$) to the $^3P_0$ state (in collisions with background Hg($6s\ ^1S_0$)) that were measured by Waddell and Hurst[16] and Stock et al.[17] Values reported in refs 16 and 17 range between 9×10^{-14} and 3×10^{-13} cm^3•s^{-1}.

The solid curve in Figure 5, the least squares fit of a second order polynomial in [Hg] (eq 3) to the data, yields k_2 as (4.5 ± 3.0) $\times 10^{-15}$ cm^3•s^{-1} and k_3 as (1.8 ± 0.4) $\times 10^{-33}$ cm^6•s^{-1}. Also, the [Hg] $\rightarrow 0$ limit of the polynomial is (6.4 ± 0.6) $\times 10^4$ s^{-1} which corresponds to a lifetime of 15.8 ± 1.5 μs. To our knowledge, no measurements or theoretical estimates for the Hg_2 (AO_g^+) state quenching rate constants are available in the literature. However, Stock and co-workers[17] have measured the binary collisional rate constant for quenching of the Hg ($6p\ ^3P_0$) state to be 4×10^{-14} cm^3•s^{-1}, which is an order of magnitude larger than the Hg_2 (A) two body quenching rate constant measured in these experiments. Also, on the basis of experiments and modeling involving a DC Hg discharge, Mosburg and Wilke[2] concluded that the three body rate constant for Hg_3 formation (from the dimer) is 20−1500 times *larger* than the corresponding three body rate constant for the production of Hg_2* (where the asterisk denotes an electronic excited state) from Hg ($6p\ ^3P_0$) atoms. When combined with the rate constant measured by Stock et al.[17] for quenching of Hg ($6p\ ^3P_0$) by three body collisions with background Hg, the result of ref 2 suggests Hg_2* three body quenching rate constants in the range of $\sim 3 \times 10^{-30}$ to 2×10^{-28} cm^6•s^{-1} which are at least 3 orders of magnitude larger than the value proposed here (1.8×10^{-33} cm^6•s^{-1}).

In ref 18, radiative decay of the heteronuclear HgCd (A1) population was monitored and a two body collisional rate constant of $\sim 1.2 \times 10^{-13}$ cm^3•s^{-1} was inferred from the data. This rate constant presumably reflects collisional mixing between excimer excited states and is, understandably, considerably larger than k_2. In contrast, the present experiments monitor the temporal history of the $O_g^{\pm}$ states which lie ~ 0.2 eV below the lowest 1_g state of Hg_2 and ~ 0.4 eV below the 1_u state which is radiatively coupled to ground by dipole-allowed transitions and, as noted earlier, is the source of the bound → free ultraviolet continuum. For the highest temperatures examined in these experiments (~ 600 K), therefore, $T_e(1_u) - T_e(O_g^{\pm}) \sim 8$ kT. One concludes that the AO_g^+ population is relatively isolated collisionally from the radiating 1_u state and that the data of Figure 5 present an accurate picture of the temporal decay of the coupled $O_g^{\pm}$ populations.

Unfortunately, analogous constants for other structurally similar diatomics such as the rare gas dimers, Cd_2 or Zn_2, also do not appear to be available but two body quenching of the rare gas halides by the rare gases is characterized by rate constants of typically 10^{-11}−10^{-12} cm^3•s^{-1}.[19] Similarly, three body rate constants for quenching of the rare gas fluoride diatomics [$RF(B^2\Sigma_{1/2}^+)$, R = Ar, Kr, or Xe] by the rare gases range from $\sim 2 \times 10^{-32}$ cm^6•s^{-1} (for XeF(B) + 2Ar → products) to $\sim 5 \times 10^{-31}$ cm^6•s^{-1} (for KrF ($B^2\Sigma$) + 2Kr). These values are also 1−2 orders of magnitude larger than the Hg_2 (A) + 2Hg → products reaction rate reported here.

One general comment regarding the [Hg] → 0 limit of the data of Figure 5 should be made. Of course, AO_g^+−XO_g^+ dipole transitions are forbidden by the u ↔ g, g ↛ g, u ↛ u selection rule for electronic transitions. Furthermore, AO_g^+−XO_g^+ is correlated, in the separated atom limit, with the $6p\ ^3P_0$−$6s\ ^1S_0$ transition of atomic Hg—a transition which is also dipole-forbidden by spin and angular momentum considerations. Wexler et al.[20] measured the Hg ($6\ ^3P_0$−$6\ ^1S_0$) A coefficient to be 0.69 s^{-1}, which suggests that $A(R)$ for the Hg-($^3P_0$)−Hg interaction potential rises by approximately 4 orders of magnitude between the separated limit and R_e for the AO_g^+ state. Ample precedent for this behavior exists for other diatomic species. One notable example is the alkali metal−rare gas molecular transitions ($^2\Sigma$−$^2\Sigma$) associated, in the separated atom limit, with $^2S_{1/2}$−$^2S_{1/2}$ transitions of the alkali

atom which are dipole-forbidden. Experiments[21] support theoretical predictions[22,23] that the oscillator strength for the $^2\Sigma \leftarrow {}^2\Sigma$ transition of CsXe, for example, that is correlated with the single-photon-forbidden 7s $^2S_{1/2} \leftarrow$ 6s $^2S_{1/2}$ transition of Cs increases by more than 8 orders of magnitude as the interatomic separation falls from ~25 to ~4 Å.

D. Conclusions

The rate constants for quenching of Hg_2 (AO_g^+) in two and three body collisions with background Hg ($6\ ^1S_0$) atoms have been measured in laser pump−probe experiments. Both rate constants, $k_2 = (4.5 \pm 3.0) \times 10^{-15}$ cm^3•s^{-1}, and $k_3 = (1.8 \pm 0.4) \times 10^{-33}$ cm^6•s^{-1}, are smaller than those typical of rare gas halide excimer quenching constants, but comparison with corresponding rate constants for homologous diatomics (Cd_2, Zn_2) must await further experiments.

Acknowledgment. The technical assistance of J. Gao, C. Herring, K. Kuehl, and K. Voyles is gratefully acknowledged. This work was supported by the U.S. Air Force Office of Scientific Research and the National Science Foundation.

References and Notes

(1) Mies, F. H.; Stevens, W. J.; Krauss, M. *J. Mol. Spectrosc*. **1978**, *72*, 303.
(2) Mosburg, E. R., Jr.; Wilke, M. D. *J. Chem. Phys*. **1977**, *66*, 5682.
(3) Ehrlich, D. J.; Osgood, R. M., Jr. *IEEE J. Quantum Electron*. **1979**, *QE−15*, 301.
(4) Figen, Z. G.; Gao, J.; Eden, J. G. Unpublished work.
(5) Niefer, R.; Atkinson, J. B.; Krause, L. *J. Phys. B* **1983**, *16*, 3531.
(6) Supronowicz, J.; Niefer, R. J.; Atkinson, J. B.; Krause, L. *J. Phys. B* **1986**, *19*, 1153; **1986**, L717.
(7) Niefer, R. J.; Supronowicz, J.; Atkinson, J. B.; Krause, L. *Phys. Rev. A* **1987**, *35*, 4629.
(8) Kedzierski, W.; Atkinson, J. B.; Krause, L. *Opt. Lett*. **1989**, *14*, 607.
(9) Kedzierski, W.; Supronowicz, J.; Atkinson, J. B.; Baylis, W. E.; Krause, L.; Couty, M.; Chambaud, G. *Chem. Phys. Lett*. **1990**, *175*, 221.
(10) Kedzierski, W.; Supronowicz, J.; Czajkowski, A.; Atkinson, J. B.; Krause, L. *J. Mol. Spectrosc*. **1995**, *173*, 510.
(11) Ehrlich, D. J.; Osgood, R. M., Jr., *Phys. Rev. Lett*. **1978**, *41*, 547; *Chem. Phys. Lett*. **1979**, *61*, 150.
(12) Rodriguez, G.; Eden, J. G. *J. Chem. Phys*. **1991**, *95*, 5539.
(13) Drullinger, R. E.; Hessel, M. M.; Smith, E. W. *J. Chem. Phys*. **1977**, *66*, 5656.
(14) Marvet, U.; Dantus, M. *Chem. Phys. Lett*. **1995**, *245*, 393.
(15) Dolg, M.; Flad, H.-J. *J. Phys. Chem*. **1996**, *100*, 6147.
(16) Waddell, B. V.; Hurst, G. S. *J. Chem. Phys*. **1970**, *53*, 3892.
(17) Stock, M.; Smith, E. W.; Drullinger, R. E.; Hessel, M. M. *J. Chem. Phys*. **1977**, *67*, 2463.
(18) Supronowicz, J.; Petro, D.; Atkinson, J. B.; Krause, L. *Phys. Rev. A* **1994**, *50*, 2161.
(19) Brau, C. A. In *Excimer Lasers*; 2nd ed.; Rhodes, C. K., Ed.; Springer: Berlin, 1984; pp 87−137.
(20) Wexler, B. L.; Wilcomb, B. E.; Djeu, N. *J. Opt. Soc. Am*. **1980**, *70*, 863.
(21) Tam, A.; Moe, G.; Park, W.; Happer, W. *Phys. Rev. Lett*. **1975**, *35*, 85. Eden, J. G.; Cherrington, B. E.; Verdeyen, J. T. *IEEE J. Quantum Electron*. **1976**, *QE−12*, 698.
(22) Pascale, J. *J. Chem. Phys*. **1977**, *67*, 204.
(23) Pascale, J.; Vandeplanque, J. *J. Chem. Phys*. **1974**, *60*, 2278.